Highly stable anodic green electrochromic aromatic polyamides: synthesis and electrochromic properties†

Cha-Wen Chang,[a] Guey-Sheng Liou*[a] and Sheng-Huei Hsiao[b]

Received 11th September 2006, Accepted 16th November 2006
First published as an Advance Article on the web 18th December 2006
DOI: 10.1039/b613140a

A 4-methoxy-substituted triphenylamine containing the aromatic diamine, 4,4′-diamino-4″-methoxytriphenylamine (**2**), was synthesized by the caesium fluoride-mediated condensation of *p*-anisidine with 4-fluoronitrobenzene, followed by palladium-catalyzed hydrazine reduction of the dinitro intermediate. A series of new polyamides with pendent 4-methoxy-substituted triphenylamine (TPA) units having inherent viscosities of 0.27–1.39 dL g^{-1} were prepared *via* the direct phosphorylation polycondensation of various dicarboxylic acids and the diamine (**2**). All the polymers were readily soluble in many organic solvents, such as *N*-methyl-2-pyrrolidinone (NMP) and *N*,*N*-dimethylacetamide (DMAc), and could be solution-cast into tough and flexible polymer films. These aromatic polyamides had useful levels of thermal stability associated with their relatively high softening temperature (242–282 °C), 10% weight-loss temperatures in excess of 470 °C, and char yields at 800 °C in nitrogen higher than 60%. The hole-transporting and electrochromic properties are examined by electrochemical and spectroelectrochemical methods. Cyclic voltammograms of the polyamide films cast onto an indium-tin oxide (ITO)-coated glass substrate exhibited reversible oxidation at 0.73–0.79 V *versus* Ag/AgCl in acetonitrile solution, and revealed excellent stability of electrochromic characteristics with a color change from colorless to green at applied potentials ranging from 0.00 to 1.05 V. These anodically polymeric electrochromic materials not only showed excellent reversible electrochromic stability with good green coloration efficiency (CE = 374 cm^2 C^{-1}) but also exhibited high contrast of optical transmittance change (ΔT %) up to 85% at 787 nm and 30% at 391 nm. After over 1000 cyclic switches, the polymer films still exhibited excellent stability of electrochromic characteristics.

Introduction

Electrochromism can be defined as the reversible change in optical properties of a material resulting from electrochemically induced redox states. Color changes are commonly between a transparent state, where the chromophore only absorbs in the UV region, and a colored state, or between two colored states in a given electrolyte solution. The electrochromic material may exhibit several colors and be termed polyelectrochromic. Electrochromic anti-glare car rear-view mirrors have already been commercialized, with other proposed applications of electrochromic materials including their use in controllable light-reflective or light-transmissive devices for optical information and storage, sunglasses, protective eyewear for the military, controllable aircraft canopies, and glare-reduction systems for offices and smart windows for use in cars and buildings.[1–3]

The first studies and commercial interests in electrochromic materials started with inorganic compounds such as tungsten trioxide (WO_3) and iridium dioxide (IrO_2).[4] Later, organic materials (*i.e.*, viologens, metallophthalocyanines and conjugated polymers) have received more attention than inorganics for electrochromic applications because of the different colors observed with these compounds while switching among their redox states.[1,5,6] Although conjugated polymers (CPs) in particular have several advantages over inorganic compounds, *i.e.*, outstanding coloration efficiency, fast switching ability, high stability, fine-tuning of the band gap (and the color) through chemical structure modification, multiple colors with the same material,[7] thin film flexibility and cost effectiveness, they have not received enough attention in terms of applications. One of the main reasons for this was the deficient third leg (green) of color space in conjugated polymers (CPs). Until the first report about a green-colored neutral conjugated polymer (CP) was published,[8] researches on conjugated polymers (CPs) as cathodic electrochromics mainly focused on red and blue colors. For green color, at least two chromophores are required that absorb at red and blue wavelengths in the neutral form, and should also deplete together when the polymer is oxidized.

Wholly aromatic polyamides are characterized as highly thermally stable polymers with a favorable balance of physical and chemical properties. However, rigidity of the backbone and strong hydrogen bonding results in high melting or glass-transition temperatures (T_gs) and limited solubility in most organic solvents.[9,10] These properties make them generally intractable or difficult to process, thus restricting

[a]*Department of Applied Chemistry, National Chi Nan University, 1 University Road, Puli, Nantou Hsien 54561, Taiwan, Republic of China. E-mail: gsliou@ncnu.edu.tw*
[b]*Department of Chemical Engineering, Tatung University, 40 Chungshan North Rd, 3rd Sec., Taipei 10452, Taiwan, Republic of China*
† The HTML version of this article has been enhanced with color images.

their applications. To overcome such a difficulty, polymer-structure modification becomes necessary. One of the common approaches for increasing solubility and processability of polyamides without sacrificing high thermal stability is the introduction of bulky, packing-disruptive groups into the polymer backbone.[11–18] We have reported some TPA-containing polyamides and polyimides from *N*,*N*′-bis(4-aminophenyl)-*N*,*N*′-diphenyl-1,4-phenylenediamine,[19,20] *N*,*N*′-bis(4-carboxyphenyl)-*N*,*N*′-diphenyl-1,4-phenylenediamine,[21] and 2,4-diaminotriphenylamine,[22] respectively. Because of the incorporation of bulky, three-dimensional TPA units along the polymer backbone, all the polymers were amorphous and exhibited good solubility in many aprotic solvents with excellent thin film-forming capability. Recently, we have initiated a study to obtain TPA-containing anodic electrochromic polymers which exhibited green light in the oxidized state and were transparent in the neutral state.[23–26]

The anodic oxidation pathways of TPA are well studied.[27] The electrogenerated cation radical of $TPA^{+\bullet}$ is not stable and could be dimerized to form tetraphenylbenzidine by tail to tail coupling with loss of two protons per dimer. When the phenyl groups were incorporated by electron-donating substituents at the *para*-position of TPA, the coupling reactions were greatly prevented affording stable cationic radicals.[28,29] In this article, we therefore synthesized a diamine, 4,4′-diamino-4″-methoxyltriphenylamine (**2**), and its derived polyamides containing TPA groups with an electron-rich pendent 4-methoxy phenyl ring which permits tuning of the solubility and redox potential of the polymers. The general properties such as solubility and thermal properties are described. The electrochemical and electrochromic properties of these polymers are also described herein and are compared with those of structurally related ones from 4,4′-diaminotriphenylamine.[30]

Experimental

Materials

4,4′-Diaminotriphenylamine (mp = 186–187 °C) was synthesized by hydrazine Pd/C-catalyzed reduction of 4,4′-dinitrotriphenylamine resulting from the condensation of aniline with 4-fluoronitrobezene in the presence of caesium fluoride (CsF) according to a previously reported procedure.[30] *N*,*N*-Dimethylacetamide (DMAc) (Tedia), *N*,*N*-dimethylformamide (DMF) (Acros), dimethyl sulfoxide (DMSO) (Tedia), *N*-methyl-2-pyrrolidinone (NMP) (Tedia), pyridine (Py) (Tedia), and triphenyl phosphite (TPP) (Acros) were used without further purification. Commercially available dicarboxylic acids such as adipic acid (**Ia**) (Showa), succinic acid (**Ib**) (Acros), *trans*-1,4-cyclohexanedicarboxylic acid (**Ic**), terephthalic acid (**Id**), isophthalic acid (**Ie**), 2,6-naphthalenedicarboxylic acid (**If**), 4,4′-biphenyldicarboxylic acid (**Ig**), 4,4′-oxydibenzoic acid (**Ih**), 4,4′-sulfonyldibenzoic acid (**Ii**), and 2,2-bis(4-carboxyphenyl)hexafluoropropane (**Ij**) were purchased from TCI and used as received. Tetrabutylammonium perchlorate (TBAP) (Acros) was recrystallized twice by ethyl acetate under a nitrogen atmosphere and then dried *in vacuo* prior to use. All other reagents were used as received from commercial sources.

Synthesis of monomer

4,4′-Dinitro-4″-methoxytriphenylamine (1). A mixture of 15.20 g (0.10 mol) of caesium fluoride in 90 mL dimethyl sulfoxide (DMSO) was stirred at room temperature. To the mixture 5.02 g (0.04 mol) of *p*-anisidine and 11.68 g (0.082 mol) of 4-fluoronitrobenzene were added in sequence. The mixture was heated with stirring at 120 °C for 24 h. The mixture was poured slowly into 300 mL of stirred methanol, and the precipitated orange–red powder was collected by filtration and washed thoroughly with methanol : water (1 : 1). The product was filtered to afford 13.07 g (89% in yield) of orange–red powder. Mp: 211–212 °C measured by DSC at 10 °C min^{-1}.

IR (KBr): 1578, 1313 cm^{-1} (–NO_2 stretch). ^1H NMR (DMSO-d_6, δ, ppm): 3.79 (s, 3H, OCH_3), 7.06 (d, 2H, H_c), 7.17 (d, 4H, H_b), 7.21 (d, 2H, H_d), 8.16 (d, 4H, H_a). ^{13}C NMR (DMSO-d_6, δ, ppm): 55.6 (OCH_3), 116.0 (C^7), 121.9 (C^2), 125.7 (C^3), 129.4 (C^6), 137.0 (C^5), 141.9 (C^1), 151.9 (C^4), 158.4 (C^8). Anal. Calcd for $C_{19}H_{15}N_3O_5$ (365.35): C, 62.46%; H, 4.14%; N, 11.50%. Found: C, 62.52%; H, 4.67%; N, 11.71%.

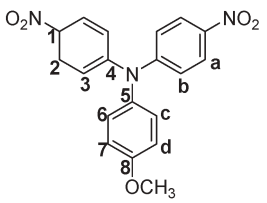

4,4′-Diamino-4″-methoxytriphenylamine (2). In a 250 mL three-neck round-bottom flask equipped with a stirring bar under nitrogen atmosphere, 7.34 g (0.020 mol) of nitro compound (**1**) and 0.13 g of 10% Pd/C were dissolved/suspended in 100 mL of ethanol. The suspension solution was heated to reflux, and 7 mL of hydrazine monohydrate was added slowly to the mixture, then the solution was stirred at reflux temperature. After a further 9 h of reflux, the solution was filtered to remove Pd/C, and the filtrate was cooled to precipitate. The product was collected by filtration and dried *in vacuo* at 80 °C to give 4.88 g (80% in yield) of light-green needles. Mp: 150–152 °C measured by DSC at 10 °C min^{-1}.

IR (KBr): 3454, 3339 cm^{-1} (N–H stretch). ^1H NMR (DMSO-d_6, δ, ppm): 3.65 (s, 3H, OCH_3), 4.82 (s, 4H, NH_2), 6.48 (d, 2H, H_a), 6.68 (d, 2H, H_b), 6.69–6.73 (m, 4H, H_c + H_d). ^{13}C NMR (DMSO-d_6, δ, ppm): 55.4 (OCH_3), 114.5 (C^7), 115.0 (C^2), 121.2 (C^6), 125.8 (C^3), 137.7 (C^4), 143.2 (C^5), 144.5 (C^1), 153.0 (C^8). Anal. Calcd for $C_{19}H_{19}N_3O$ (305.37): C, 74.73%; H, 6.27%; N, 13.76%. Found: C, 74.54%; H, 6.19%; N, 13.63%.

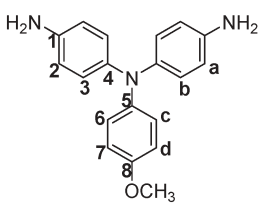

Polymer synthesis

The synthesis of polyamide **IId** is used as an example to illustrate the general synthetic route. The typical procedure

was as follows. A mixture of 0.382 g (1.25 mmol) of 4,4′-diamino-4″-methoxytriphenylamine (**2**), 0.208 g (1.25 mmol) of terephthalic acid (**Id**), 0.15 g of calcium chloride, 1.25 mL of TPP, 0.6 mL of Py, and 1.25 mL of NMP was heated with stirring at 105 °C for 3 h. The polymer solution was poured slowly into 300 mL of stirring methanol giving rise to a stringy, fiber-like precipitate that was collected by filtration, washed thoroughly with hot water and methanol successively, and dried under vacuum at 100 °C; yield: 0.538 g (99%). Reprecipitations from DMAc into methanol were carried out twice for further purification. The inherent viscosity of the obtained polyamide **IId** was 0.79 dL g^{-1}, measured at a concentration of 0.5 g dL^{-1} in NMP at 30 °C. The IR spectrum of **IId** (film) exhibited characteristic amide absorption bands at 3310 (N–H stretching), 1654 cm^{-1} (amide carbonyl). Anal. Calcd for $(C_{27}H_{21}N_3O_3)_n$ $(435.47)_n$: C, 74.47%; H, 4.86%; N, 9.65%. Found: C, 73.52%; H, 4.98%; N, 9.48%. The other polyamides were prepared by an analogous procedure.

Preparation of the films

A solution of the polymer was made by dissolving about 0.5 g of the polyamide sample in 10 mL of DMAc or NMP. The homogeneous solution was poured into a 9 cm glass Petri dish, which was placed in a 90 °C oven for 5 h to remove most of the solvent; then the semi-dried film was further dried *in vacuo* at 170 °C for 8 h. The obtained films were about 40–60 μm thick and were used for X-ray diffraction measurements, solubility tests, and thermal analyses.

Measurements

Infrared spectra were recorded on a PerkinElmer RXI FT-IR spectrometer. Elemental analyses were run in an Elementar Vario EL-III. ^1H and ^{13}C NMR spectra were measured on a Bruker AV-400 FT-NMR system and referenced to the DMSO-d_6 signal, and peak multiplicity was reported as follows: s, singlet; d, doublet; t, triplet; m, multiplet. The inherent viscosities were determined at 0.5 g dL^{-1} concentration using a Tamson TV-2000 viscometer at 30 °C. Wide-angle X-ray diffraction (WAXD) measurements were performed at room temperature (*ca.* 25 °C) on a Shimadzu XRD-7000 X-ray diffractometer (40 kV, 20 mA), using graphite-monochromatized Cu-Kα radiation. Ultraviolet-visible (UV-vis) spectra of the polymers were recorded on a Varian Cary 50 Probe spectrometer. Thermogravimetric analysis (TGA) was conducted with a PerkinElmer Pyris 1 TGA. Experiments were carried out on approximately 6–8 mg film samples heated in flowing nitrogen or air (flow rate = 20 cm^3 min^{-1}) at a heating rate of 20 °C min^{-1}. Thermomechanical analysis (TMA) was conducted with a PerkinElmer TMA 7 instrument. The TMA experiments were conducted from 50 to 350 °C at a scan rate of 10 °C min^{-1} with a penetration probe 1.0 mm in diameter under an applied constant load of 10 mN. Softening temperatures (T_ss) were taken as the onset temperatures of probe displacement on the TMA traces. Cyclic voltammetry was performed with a Bioanalytical System Model CV-27 potentiostat and a BAS X-Y recorder with ITO (polymer film area about 0.7 cm × 0.5 cm) as a working electrode and a platinum wire as an auxiliary electrode at a scan rate of 50 mV s^{-1} against a Ag/AgCl reference electrode in a solution of 0.1 M tetrabutylammonium perchlorate (TBAP) : acetonitrile (CH_3CN). Voltammograms are presented with the positive potential pointing to the left and with increasing anodic currents pointing downwards. The spectroelectrochemical cell was composed of a 1 cm cuvette, ITO as a working electrode, a platinum wire as an auxiliary electrode, and a Ag/AgCl reference electrode. Absorption spectra in spectroelectochemical analysis were measured with a HP 8453 UV-vis spectrophotometer. Photoluminescence spectra were measured with a Jasco FP-6300 spectrofluorometer. Fluorescence quantum yields (Φ_F) of the samples in NMP were measured by using quinine sulfate in 1 M H_2SO_4 as a reference standard (Φ_F = 0.546).[31] All corrected fluorescence excitation spectra were found to be equivalent to their respective absorption spectra.

Results and discussion

Monomer synthesis

An aromatic diamine with a pendent 4-methoxy-substituted triphenylamine group, 4,4′-diamino-4″-methoxytriphenylamine (mp = 150–152 °C), was prepared through the CsF-mediated nucleophilic displacement reaction of *p*-anisidine with 4-fluoronitrobenzene, followed by hydrazine Pd/C-catalyzed reduction.[32,33] The synthetic routines are outlined in Scheme 1. Due to the inherent electron-donating nature arising from the nitrogen atom through the conjugated aromatic *p*-anisidine, the compound (**1**) could be readily obtained in high purity and good yield (89%). 4,4′-Diamino-4″-methoxyltriphenylamine (**2**) could be obtained by the catalytic reduction of compound (**1**) with hydrazine monohydrate or under a hydrogen atmosphere. Elemental analysis, IR, and ^1H and ^{13}C NMR spectroscopic techniques were used to identify the structures of the intermediate compounds (**1**) and (**2**). The transformation of nitro to amino groups could be monitored by changes in the IR spectra. The nitro groups of compound (**1**) gave two characteristic bands at around 1579 cm^{-1} and 1312 cm^{-1} (–NO_2 asymmetric and symmetric stretching). After reduction, the characteristic absorptions of the nitro group disappeared and the amino group showed the

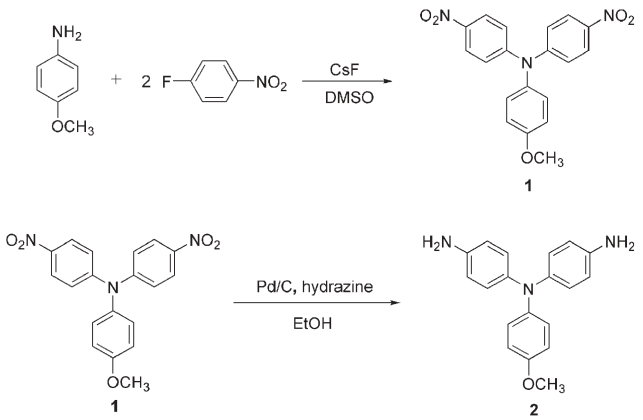

Scheme 1

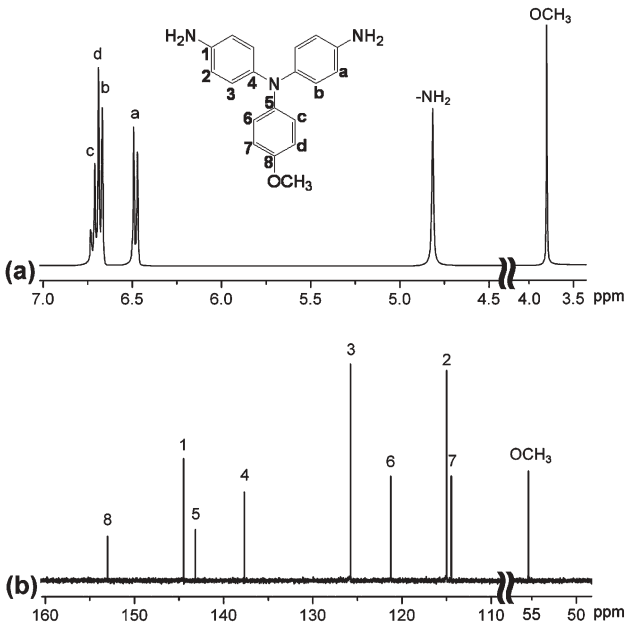

Fig. 1 (a) ^{1}H NMR and (b) ^{13}C NMR spectra of compound **2** in DMSO-d_6.

typical N–H stretching absorption pair in the region of 3300–3500 cm^{-1}. Fig. 1 illustrates the ^{1}H NMR and ^{13}C NMR spectra of diamine (**2**). Assignments of each carbon and proton are also given in these figures, and agree well with the proposed molecular structure. The ^{1}H NMR spectra confirm that the nitro groups have been completely transformed into amino groups by the high field shift of the aromatic protons and the resonance signals at around 4.8 ppm corresponding to the amino protons.

Polymer synthesis

According to the phosphorylation technique first described by Yamazaki and coworkers,[34,35] a series of novel polyamides (**IIa–IIj**) with pendent 4-methoxy-substituted triphenylamine units were synthesized from the diamine (**2**) and various dicarboxylic acids *via* solution polycondensation using TPP and Py as condensing agents as shown in Scheme 2. All the polymerization proceeded homogeneously throughout the

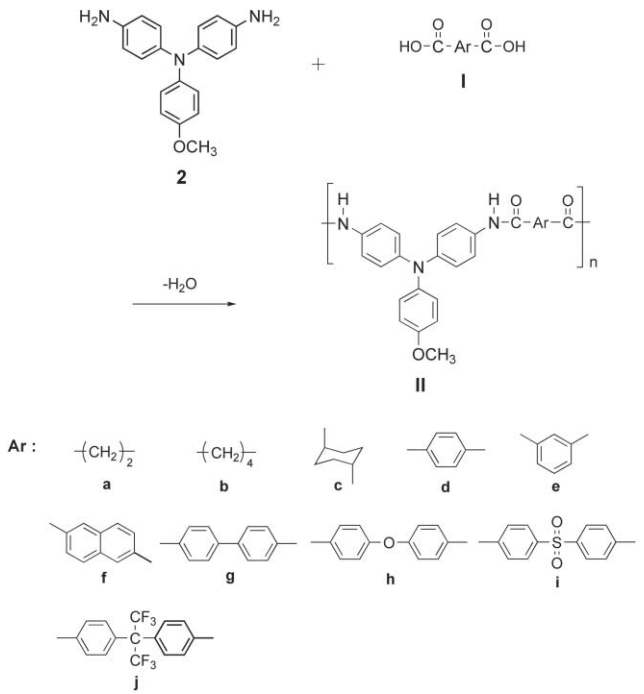

Scheme 2 Synthesis of polyamides by direct polycondensation reaction.

reaction and afforded clear and highly viscous polymer solutions, which precipitated in a tough, fiber-like form when the resulting polymer solutions were slowly poured into stirring methanol. As shown in Table 1, the obtained polyamides had inherent viscosities (η_{inh}) in the range 0.27–1.39 dL g^{-1}, and could be solution-cast into flexible and tough films indicating the formation of high molecular weight polymers.

The elemental analyses were in a good agreement with the proposed structures. The formation of polyamides was also confirmed by IR and NMR spectroscopy. Fig. 2 shows a typical IR spectrum for polyamide **IId**. The characteristic IR absorption bands of the amide group were around 3310 (N–H stretching) and 1654 cm^{-1} (amide carbonyl). Fig. 3 shows a typical set of ^{1}H and ^{13}C NMR spectra of polyamide **IId** in DMSO-d_6; all the peaks could be readily assigned to the

Table 1 Inherent viscosities and thermal properties of polyamides

Polymer	η_{inh}[a]/dL g^{-1}	T_s/°C[b]	T_d at 5% weight loss/°C[c]		T_d at 10% weight loss/°C[c]		Char yield (wt%)[d]
			N_2	Air	N_2	Air	N_2
IIa	0.27	165	350	345	375	375	35
IIb	0.53	170	390	400	400	415	25
IIc	0.68	259	415	395	445	445	40
IId	0.79	248	465	430	515	465	63
IIe	0.44	252	445	445	485	495	67
IIf	0.93	282	440	455	470	495	66
IIg	1.39	276	470	470	505	520	65
IIh	0.60	242	455	455	495	500	69
IIi	0.72	277	455	465	485	485	64
IIj	0.39	263	440	470	500	515	62

[a] Measured at a polymer concentration of 0.5 g dL^{-1} in NMP at 30 °C. [b] Softening temperature measured by TMA with a constant applied load of 10 mN at a heating rate of 10 °C min^{-1}. [c] Decomposition temperature, recorded *via* TGA at a heating rate of 20 °C min^{-1} and a gas-flow rate of 30 cm^{3} min^{-1}. [d] Residual weight percentage at 800 °C in nitrogen.

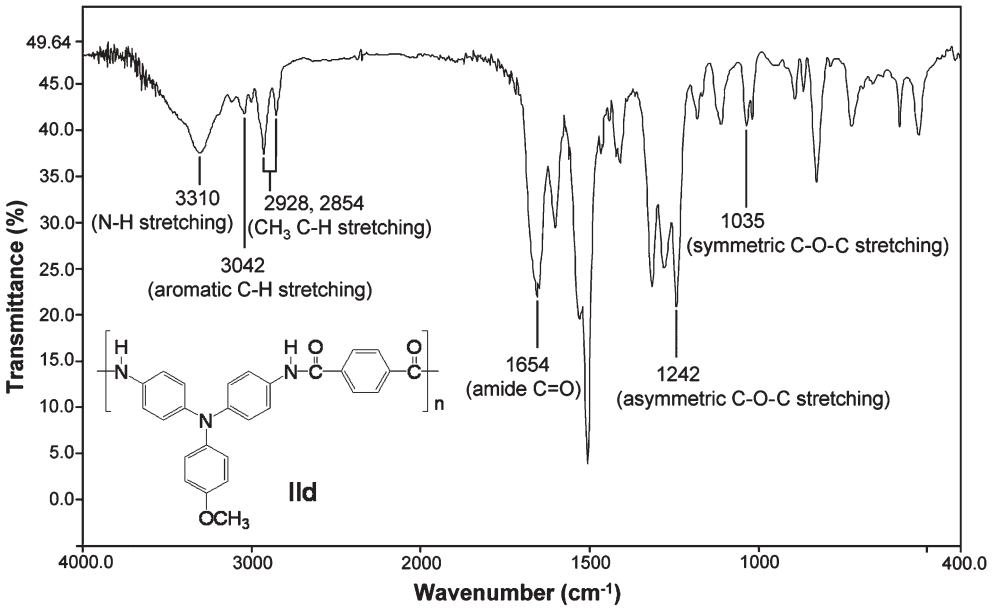

Fig. 2 IR spectrum (film) of polyamide **IId**.

hydrogen and carbon atoms of the recurring unit. The resonance peaks appearing at 10.33 ppm in the ^{1}H NMR spectrum and at 164.3 ppm in the ^{13}C NMR spectrum also support the formation of amide linkages.

Basic characterization

The solubility behavior of polyamides was tested qualitatively, and the results are summarized in Table 2. All the polyamides were highly soluble in polar solvents such as NMP, DMAc, DMF, and DMSO, and the enhanced solubility could be attributed to the introduction of the bulky pendent methoxy-substituted TPA moiety into the repeat unit. Thus, the excellent solubility makes these polymers potential candidates for practical applications by spin- or dip-coating processes.

The wide-angle X-ray diffraction (WAXD) patterns of the polyamides given in Fig. 4 indicate that the polymers were essentially amorphous, revealing that the methoxy-substituted TPA-containing polyamides do not form a well-packed structure. The amorphous nature of these polyamides was reflected not only in their good solubility but also agreed with the UV-vis data of the polymers, which show that the UV-vis absorption peaks of the polymers do not shift from the solutions to the films, implying that there is no significant π–π interaction aggregation between the polymer chains.

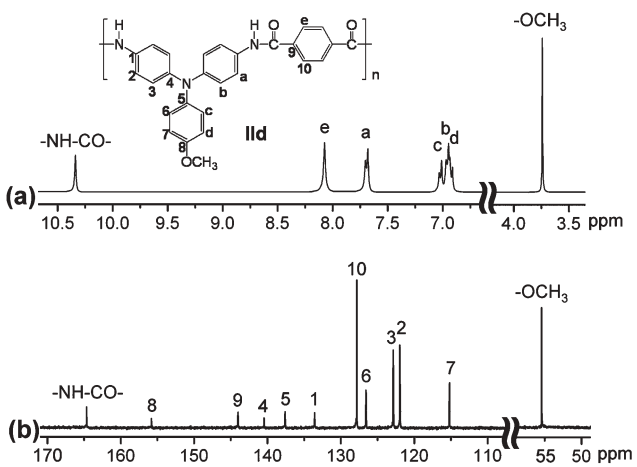

Fig. 3 (a) ^{1}H NMR and (b) ^{13}C NMR spectra of polyamide **IId** in DMSO-d_6.

The thermal properties of the polyamides were investigated by TGA and TMA. The results are summarized in Table 1. Typical TGA curves of representative polyamide **IIj** in both air and nitrogen atmospheres are shown in Fig. 5. All the aromatic polyamides exhibited good thermal stability with insignificant weight loss up to 430 °C in nitrogen. Their 10% weight-loss temperatures in nitrogen and air were recorded at 475–505 and 465–520 °C, respectively. The carbonized residue (char yield) of these aromatic polymers was more than 63% at 800 °C in nitrogen atmosphere. The high char yields of these polymers could be ascribed to their high aromatic content. The softening temperature (T_s) values of the polymer films were

Table 2 Solubility[a] of polyamides

	Solvents						
Polymer	NMP	DMAc	DMF	DMSO	*m*-cresol	THF	$CHCl_3$
IIa	++	++	++	++	++	—	—
IIb	++	++	++	++	++	—	—
IIc	++	++	++	++	++	—	—
IId	++	++	++	++	+	—	—
IIe	++	++	++	++	++	—	—
IIf	++	++	++	++	+	—	—
IIg	++	++	++	++	+	—	—
IIh	++	++	++	++	+	—	—
IIi	++	++	++	++	+	—	—
IIj	++	++	++	++	++	—	—

[a] Qualitative solubility was tested with 1 mg of a sample in 1 mL of stirred solvent. ++, soluble at room temperature; +, soluble on heating; ±, partially soluble; S, swelling; —, insoluble even on heating.

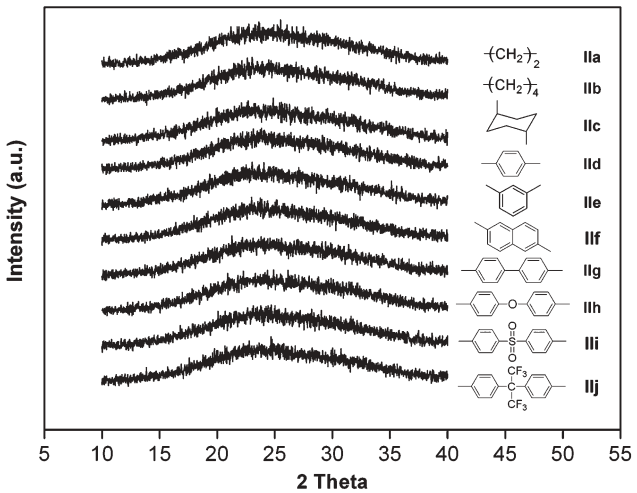

Fig. 4 WAXD pattern of polyamide films.

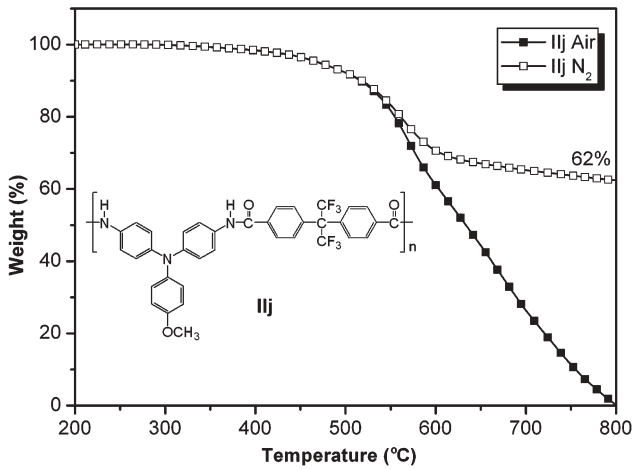

Fig. 5 TGA thermograms of polyamide **IIj** at a scan rate of 20 °C min^{-1}.

determined from the onset temperature of the probe displacement on the TMA trace, and observed in the range 165–282 °C, depending on the structure of diacid component, and decreased with decreasing rigidity of the polymer backbone, or with the introduction of flexible linkages in the polymer main chain. A typical TMA thermogram for polyamide **IIi** is illustrated in Fig. 6.

Optical and electrochemical properties

The optical and electrochemical properties of the polyamides were investigated by UV-vis and photoluminescence spectroscopy, and cyclic voltammetry. The results are summarized in Table 3. The UV-vis absorption of these polymers exhibited strong absorption at 262–370 nm in NMP solutions, which are assignable to a π–π* transition resulting from the conjugation between the aromatic rings and nitrogen atoms. The UV-vis absorption of methoxy-substituted TPA-based polyamide films **IIa–IIj** also showed similar single absorbance at 264–377 nm in the solution state. Fig. 7 shows the UV-vis absorption and photoluminescence spectra of polyamides **IIa**,

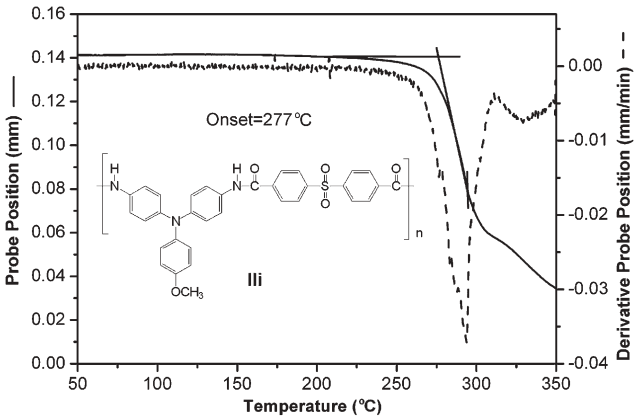

Fig. 6 TMA curve of polyamide **IIi** with a heating rate of 10 °C min^{-1}.

IIb, and **IIc** in NMP (concentration: 1×10^{-5} mol L^{-1}). Aromatic–aliphatic polyamides **IIa–IIc** and aromatic polyamides **IId–IIj** in NMP solution exhibited fluorescence emission maxima at 394–396 nm and 444–460 nm with quantum yields ranging from 1.85% for **IIa** to 3.63% for **IIc**, respectively. The blue shift and higher fluorescence quantum yield of aromatic–aliphatic polyamides **IIa–IIc** compared with aromatic polyamides **IId–IIj** could be attributed to the effectively reduced conjugation and capability of charge transfer complex formation by aliphatic diacids with the electron-donating diamine moiety in comparison with that of the strongly electron-accepting aromatic diacids. The cutoff wavelengths (absorption edge) from UV-vis transmittance spectra were in the range 358–447 nm. Because of the lower capability of charge transfer, polyamides **IIa–IIc** showed a light color and high optical transparency with cutoff wavelengths in the range 358–360 nm.

The electrochemical behavior of the polyamide **II** series was investigated by cyclic voltammetry conducted by film cast on an ITO-coated glass substrate as the working electrode in dry acetonitrile (CH_3CN) containing 0.1 M of TBAP as an electrolyte under nitrogen atmosphere. The typical cyclic voltammograms for TPA-containing polyamide **IIh** (with 4-methoxy-substituted) and **IIh′** (without 4-methoxy-substituted) are shown in Fig. 8 for comparison. Electrochemical oxidation (or p-doping) of polymer **IIh** starts at about 0.62 V (E_{onset}) with a reversible oxidation process at $E_{1/2}$ (average potential of the redox couple peaks) 0.76 V *versus* Ag/AgCl. After 1000 continuous cyclic scans between 0.0 to 1.05 V, the polymer films still exhibited excellent electrochemical stability. The oxidation of polyamide **IIh** occurred at the nitrogen center of the TPA unit, which is incorporated by electron-donating methoxyl substituents at the *para*-position of phenyl rings in a propeller-like geometry. The introduction of electron-donating methoxyl substituents into the *para*-position of TPA not only greatly stabilize the cationic radicals but also lower the oxidation potentials of the electroactive polyamides **II** as compared with the corresponding polyamides **II′** without methoxyl substituents. The energy of the highest occupied molecular orbital (HOMO) and lowest unoccupied molecular orbital (LUMO) levels of the investigated polyamides could be determined from the oxidation onset or half-wave potentials

Table 3 Optical and electrochemical properties for polyamides

	Solution λ/nm[a]			film λ/nm				$E_{1/2}$/V (*vs.* Ag/AgCl in CH_3CN)			HOMO[f]/eV		LUMO[g]/eV	
Index	Abs. max	PL max	Φ_F (%)[b]	λ_0[c]	Abs. max	Abs. onset	PL max[d]	$E_{1/2}$	E_{onset}	E_g[e]/eV	$E_{1/2}$	E_{onset}	$E_{1/2}$	E_{onset}
IIa	263	396	1.85	360	264	371	395	0.76	0.60	3.34	5.08	4.96	1.74	1.62
IIb	263	394	2.18	360	265	367	399	0.75	0.60	3.37	5.07	4.96	1.70	1.59
IIc	262	396	3.63	358	264	362	390	0.79	0.60	3.43	5.11	4.96	1.68	1.53
IId	364	445	0.23	431	364	454	496	0.73	0.58	2.73	5.05	4.94	2.32	2.21
IIe	348	444	0.29	394	344	417	512	0.75	0.59	2.97	5.07	4.95	2.10	1.98
IIf	370	454	0.13	447	377	466	469	0.77	0.62	2.66	5.09	4.98	2.43	2.32
IIg	364	451	0.17	432	361	446	502	0.75	0.60	2.78	5.07	4.96	2.29	2.18
IIh	342	446	0.29	394	345	407	509	0.76	0.62	3.05	5.08	4.98	2.03	1.93
IIi	364	460	0.15	444	361	488	507	0.78	0.65	2.54	5.10	5.01	2.56	2.47
IIj	354	446	0.34	398	356	427	492	0.79	0.65	2.90	5.11	5.01	2.21	2.11
IIh′	336	477	2.30	391	334	409	492	0.85	0.71	3.03	5.16	5.07	2.13	2.04

[a] Spectra in NMP (1×10^{-5} mol L^{-1}). [b] The quantum yield in dilute solution was calculated in an integrating sphere with quinine sulfate as the standard (Φ_F = 0.546). [c] The cutoff wavelength from the UV-vis transmission spectra of polymer films. [d] Excited at the absorption maximum for both the solid and solution states. [e] The data were calculated by the equation: $E_g = 1240/\lambda_{onset}$ of polymer film. [f] The HOMO energy levels were calculated from cyclic voltammetry and were referenced to ferrocene (4.8 eV). [g] LUMO = HOMO – E_g.

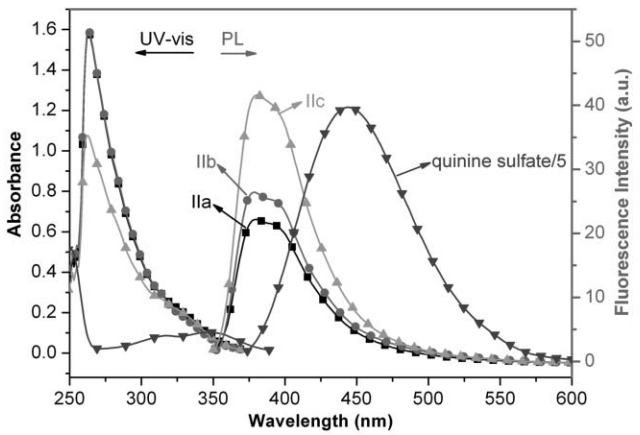

Fig. 7 UV-vis absorptions and photoluminescence (PL) spectra of polyamides **IIa**, **IIb**, **IIc** in NMP (1×10^{-5} M). Quinine sulfate dissolved in 1 M H_2SO_4 (aq.) with a concentration of 1×10^{-5} M as the standard (Φ_F = 0.546).

and the onset absorption wavelength of polymer films, and the results are also listed in Table 3. For example, the oxidation half-wave potential for polyamide **IIh** has been determined as 0.76 V (E_{onset} = 0.62 V) *vs* Ag/AgCl. The external ferrocene/ferrocenium (Fc/Fc^+) redox standard $E_{1/2}$ (Fc/Fc^+) is 0.48 V *vs* Ag/AgCl in CH_3CN. Assuming that the HOMO energy for the Fc/Fc^+ standard is 4.80 eV with respect to the zero vacuum level, the HOMO energy for polyamide **IIh** has been evaluated to be 5.08 eV.

Electrochromic characterization

Electrochromism of the polyamide thin films was examined by an optically transparent thin-layer electrode (OTTLE) coupled with UV-vis spectroscopy. The electrode preparation and solution condition were identical to those used in cyclic voltammetry. The typical electrochromic transmittance spectra of polyamide **IIh** are shown in Fig. 9. When the applied potentials increased positively from 0.00 to 0.95 V, the peak of absorption at 345 nm, characteristic for the neutral form polyamide **IIh**, decreased gradually, while two new bands grew

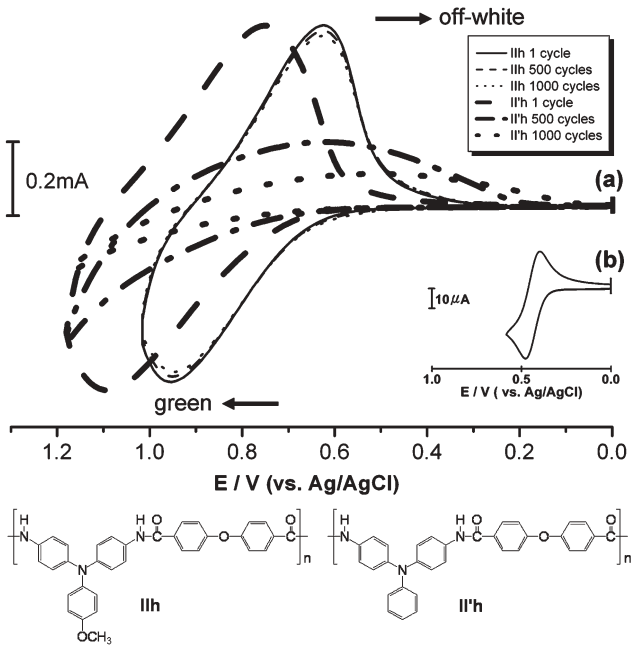

Fig. 8 Cyclic voltammograms of (a) polyamides **IIh** and **IIh′** film onto an indium-tin oxide (ITO)-coated glass substrate over 1000 cyclic scans (b) ferrocene in CH_3CN containing 0.1 M TBAP at scan rate = 0.05 V s^{-1}.

up at 391 and 787 nm, respectively. The new spectral patterns were assigned as those of the cationic radical polyamide **IIh**, formed by electron removal from the lone pair on the nitrogen atom on the TPA structure causing the structure to flatten off and delocalise, so can absorb at longer wavelengths. Meanwhile, the color of the **IIh** film changed from colorless to green with high contrast of optical transmittance change (ΔT%) up to 85% at 787 nm and 30% at 391 nm (as shown in Fig. 9).

The color switching times were estimated by applying a potential step, and the absorbance profiles were followed (Fig. 10). The switching time was defined as the time required to reach 90% of the full change in absorbance after the

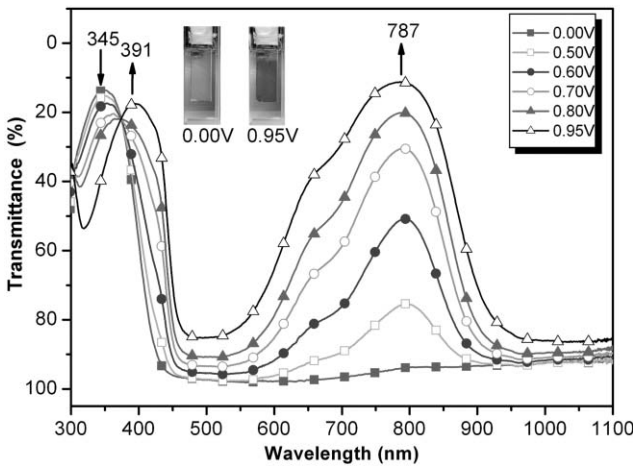

Fig. 9 Electrochromic behavior of polyamide **IIh** thin film (in CH_3CN with 0.1 M TBAP as the supporting electrolyte) at 0.00 V (■), 0.50 V (□), 0.60 V (●), 0.70 V (○), 0.80 V (▲), 0.95 V (△).

switching of the potential. Thin films from polyamide **IIh** would require 4.5 s at 0.95 V for switching absorbance at 391 and 787 nm and 1.5 s for bleaching. The color switching times of polyamide **IIh** are also shown in Fig 10. After over 1000 cyclic scans, the polymer films still exhibited good stability of electrochromic characteristics. The high electrochromic

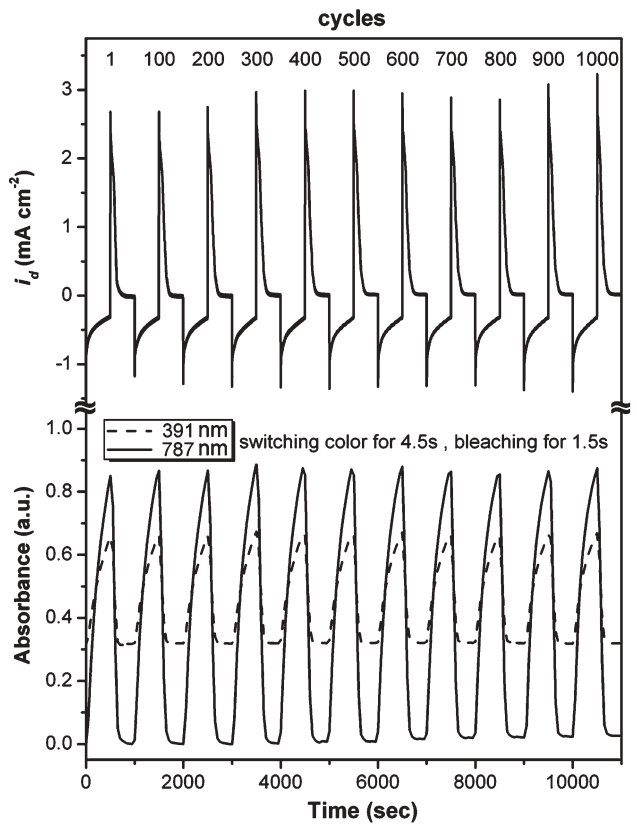

Fig. 10 Potential step absorptometry and current consumption of polyamide **IIh** (in CH_3CN with 0.1 M TBAP as the supporting electrolyte) by applying a potential step (0.00 V ⇒ 0.95 V, coated area: 1 cm^2) and cycle time of 10 s for coloration efficiency from 374 cm^2 C^{-1} (1st cycle) to 330 cm^2 C^{-1} (1000th cycle).

Table 4 Optical and electrochemical data collected for polyamide **IIh** coloration efficiency measurements

Cycle	ΔA	Q/mC cm^{-2}	η/cm^2 C^{-1}	Decay (%)
1	0.852	2.28	374	0
100	0.866	2.45	353	5.6
200	0.867	2.46	352	5.9
300	0.891	2.55	349	6.7
400	0.867	2.49	348	7.0
500	0.873	2.53	345	7.8
600	0.863	2.51	344	8.0
700	0.847	2.47	343	8.3
800	0.835	2.44	342	8.6
900	0.844	2.56	330	11.7
1000	0.851	2.58	330	11.8

coloring efficiency [$\eta = \Delta A/Q$ where ΔA is the optical absorbance change, and Q (minicoulombs of charge per square centimetre, mq cm^{-2}) is the injected/ejected charge as a function of electrode area for switching an electrochromic device from one state to another] ranging from 374 cm^2 C^{-1} for the first cycle to 330 cm^2 C^{-1} for the thousandth cycle and decay of the polyamide **IIh** were calculated[36] and the results are summarized in Table 4.

Conclusions

A series of highly stable anodic green electrochromic polyamides with high contrast of optical transmittance change (ΔT%) up to 85% at 787 nm and 30% at 391 nm have been readily prepared from the diamine, 4,4′-diamino-4″-methoxytriphenylamine, and various aromatic dicarboxylic acids *via* direct phosphorylation polycondensation. Because of the incorporation of electron-donating methoxy substituents at the *para*-position of TPA, not only the electrochemical oxidative coupling reactions could be greatly prevented but also lower the oxidation potentials of the electroactive polyamides. In addition to the enhanced solubility and excellent thin film formability, high T_s values, and good thermal stability, these anodically polymeric electrochromic materials also showed excellent continuous cyclic stability of electrochromic characteristics with good coloration efficiency from 374 cm^2 C^{-1} for first cycle to 330 cm^2 C^{-1} for thousandth cycle, changing color from the colorless neutral form to the green oxidized forms when scanning potentials increased positively from 0.00 to 0.95 V. After over 1000 cyclic switches, the polymer films still exhibited excellent reversibility of electrochromic characteristics. Thus, the 4-methoxy-substituted TPA-based polyamides could be good candidates as anodic electrochromic materials due to their proper oxidation potentials, excellent electrochemical and thermal stability.

Acknowledgements

The authors are grateful to the National Science Council of the Republic of China for financial support of this work.

References

1 P. M. S. Monk, R. J. Mortimer and D. R. Rosseinsky, *Electrochromism: Fundamentals and Applications*, VCH, Weinheim, 1995.

2 M. Green, *Chem. Ind.*, 1996, **17**, 641.
3 R. J. Mortimer, *Chem. Soc. Rev.*, 1997, **26**, 147.
4 W. C. Dautremont-Smith, *Displays*, 1982, **3**, 3.
5 R. J. Mortimer, *Electrochim. Acta*, 1999, **44**, 2971.
6 K. Bange and T. Gambke, *Adv. Mater.*, 1990, **2**, 10.
7 (*a*) A. Kumar, D. M. Welsh, M. C. Morvant, F. Piroux, K. A. Abboud and J. R. Reynolds, *Chem. Mater.*, 1998, **10**, 896; (*b*) G. Sonmez, I. Schwandemann, P. Schottland, K. Zong and J. R. Reynolds, *Macromolecules*, 2003, **36**, 639; (*c*) S. A. Sapp, G. A. Sotzing and J. R. Reynolds, *Chem. Mater.*, 1998, **10**, 2101; (*d*) B. C. Thompson, P. Schottland, K. Zong and J. R. Reynolds, *Chem. Mater.*, 2000, **12**, 1563.
8 (*a*) G. Sonmez, C. K. F. Shen, Y. Rubin and F. Wudl, *Angew. Chem., Int. Ed.*, 2004, **43**, 1498; (*b*) G. Sonmez, H. B. Sonmez, C. K. F. Shen, R. W. Jost, Y. Rubin and F. Wudl, *Macromolecules*, 2005, **38**, 669; (*c*) G. Sonmez, H. B. Sonmez, C. K. F. Shen and F. Wudl, *Adv. Mater.*, 2004, **16**, 1905.
9 P. E. Cassidy, *Thermally Stable Polymers*, Marcel Dekker, New York, 1980.
10 H. H. Yang, *Aromatic High-Strength Fibers*, Wiley, New York, 1989.
11 Y. Imai, *High Perform. Polym.*, 1995, **7**, 337.
12 Y. Imai, *React. Funct. Polym.*, 1996, **30**, 3.
13 S. H. Hsiao and C. T. Li, *Macromolecules*, 1998, **31**, 7213.
14 G. S. Liou, *J. Polym. Sci., Part A: Polym. Chem.*, 1998, **36**, 1937.
15 G. C. Eastmond, J. Paprotny and R. S. Irwin, *Polymer*, 1999, **40**, 469.
16 G. C. Eastmond, M. Gibas and J. Paprotny, *Eur. Polym. J.*, 1999, **35**, 2097.
17 D. S. Reddy, C. H. Chou, C. F. Shu and G. H. Lee, *Polymer*, 2003, **44**, 557.
18 B. Y. Myung, C. J. Ahn and T. H. Yoon, *Polymer*, 2004, **45**, 3185.
19 G. S. Liou, S. H. Hsiao, M. Ishida, M. Kakimoto and Y. Imai, *J. Polym. Sci., Part A: Polym. Chem.*, 2002, **40**, 2810.
20 G. S. Liou, S. H. Hsiao, M. Ishida, M. Kakimoto and Y. Imai, *J. Polym. Sci., Part A: Polym. Chem.*, 2002, **40**, 3815.
21 G. S. Liou and S. H. Hsiao, *J. Polym. Sci., Part A: Polym. Chem.*, 2003, **41**, 94.
22 S. H. Hsiao, C. W. Chen and G. S. Liou, *J. Polym. Sci., Part A: Polym. Chem.*, 2004, **42**, 3302.
23 S. H. Cheng, S. H. Hsiao, T. H. Su and G. S. Liou, *Macromolecules*, 2005, **38**, 307.
24 T. H. Su, S. H. Hsiao and G. S. Liou, *J. Polym. Sci., Part A: Polym. Chem.*, 2005, **43**, 2085.
25 G. S. Liou, S. H. Hsiao and T. H. Su, *J. Mater. Chem.*, 2005, **15**, 1812.
26 G. S. Liou, S. H. Hsiao and T. H. Su, *J. Polym. Sci., Part A: Polym. Chem.*, 2005, **43**, 3245.
27 E. T. Seo, R. F. Nelson, J. M. Fritsch, L. S. Marcoux, D. W. Leedy and R. N. Adams, *J. Am. Chem. Soc.*, 1966, **88**, 3498.
28 L. Hagopian, G. Kohler and R. I. Walter, *J. Phys. Chem.*, 1967, **71**, 2290.
29 A. Ito, H. Ino, K. Tanaka, K. Kanemoto and T. Kato, *J. Org. Chem.*, 2002, **67**, 491.
30 Y. Oishi, H. Takado, M. Yoneyama, M. Kakimoto and Y. Imai, *J. Polym. Sci., Part A: Polym. Chem.*, 1990, **28**, 1763.
31 J. N. Demas and G. A. Crosby, *J. Phys. Chem.*, 1971, **75**, 991.
32 Y. Nishikata, S. Fukui, M. Kakimoto, Y. Imai, K. Nishiyama and M. Fujihira, *Thin Solid Films*, 1992, **296**, 210.
33 K. Y. Chiu, T. X. Su, J. H. Li, T. H. Lin, G. S. Liou and S. H. Cheng, *J. Electroanal. Chem.*, 2005, **575**, 95.
34 N. Yamazaki, F. Higashi and J. Kawabata, *J. Polym. Sci., Polym. Chem. Ed.*, 1974, **12**, 2149.
35 N. Yamazaki, M. Matsumoto and F. Higashi, *J. Polym. Sci., Polym. Chem. Ed.*, 1975, **13**, 1375.
36 R. J. Mortimer and J. R. Reynolds, *J. Mater. Chem.*, 2005, **15**, 2226.